



## A new species of planthopper in the genus *Myxia* (Hemiptera: Auchenorrhyncha: Cixiidae) from the Reserva Privada el Silencio de Los Angeles Cloud Forest in Costa Rica

MARCO A. ZUMBADO ECHAVARRIA<sup>1</sup>, EDWIN A. BARRANTES BARRANTES<sup>2</sup>, CHARLES R. BARTLETT<sup>3</sup>, ERICKA E. HELMICK<sup>4</sup> & BRIAN W. BAHDER<sup>5</sup>

<sup>1</sup>Universidad de Costa Rica—Sede San Ramón, Departamento de Ciencias Naturales, de la Iglesia el Tremedal 400 mts al Oeste carretera hacia San Pedro, San Ramón, Alajuela, Costa Rica.

✉ [marco.zumbado@ucr.ac.cr](mailto:marco.zumbado@ucr.ac.cr); [nassua75@gmail.com](mailto:nassua75@gmail.com); <https://orcid.org/0000-0002-2591-7662>

<sup>2</sup>Universidad de Costa Rica—Sede San Ramón, Departamento de Ciencias Naturales, de la Iglesia el Tremedal 400 mts al Oeste carretera hacia San Pedro, San Ramón, Alajuela, Costa Rica.

✉ [edwin.barrantes@ucr.ac.cr](mailto:edwin.barrantes@ucr.ac.cr); [edwbarrantes@gmail.com](mailto:edwbarrantes@gmail.com); <https://orcid.org/0000-0001-9565-2105>

<sup>3</sup>University of Delaware, Department of Entomology and Wildlife Ecology, 250 Townsend Hall, Newark, DE 19716-2160, USA.

✉ [bartlett@udel.edu](mailto:bartlett@udel.edu); <https://orcid.org/0000-0001-9428-7337>

<sup>4</sup>University of Florida, Department of Entomology and Nematology—Fort Lauderdale Research and Education Center; 3205 College Ave., Davie, FL 33314-7719, USA.

✉ [ehelmick@ufl.edu](mailto:ehelmick@ufl.edu); <https://orcid.org/0000-0002-5153-0891>

<sup>5</sup>University of Florida, Department of Entomology and Nematology—Fort Lauderdale Research and Education Center; 3205 College Ave., Davie, FL 33314-7719, USA.

✉ [bbahder@ufl.edu](mailto:bbahder@ufl.edu); <https://orcid.org/0000-0002-1118-4832>

### Abstract

A new species of *Myxia* Bahder & Bartlett (Cixiidae: Cixiinae: Oecleini) is established as *Myxia baynardi* **sp. n.** collected from native palms in cloud forest habitat in Costa Rica. Placement in the genus *Myxia* is supported by molecular analysis of the cytochrome *c* oxidase subunit I (COI) and 18S loci as well as morphological characters. *Haplaxius delta* (Kramer) was collected along the Caribbean coast as a new country record for Costa Rica. Based on morphological characters observed and molecular analysis of COI and 18S, *H. delta* is herein moved to the genus *Myxia*.

**Key words:** Cixiidae, taxonomy, planthopper, palm, Costa Rica

### Resumen

Una nueva especie del género *Myxia* Bahder & Bartlett (Cixiidae: Cixiinae: Oecleini) fue encontrada en palmas nativas en el hábitat de bosque nuboso en Costa Rica. Esta nueva especie se denomina *Myxia baynardi* **sp. n.** Su colocación bajo el género *Myxia* está respaldada por el análisis molecular de la subunidad I del citocromo *c* oxidasa (COI) y los loci 18S, así como por sus caracteres morfológicos. La especie *Haplaxius delta* (Kramer) fue recolectada a lo largo de la costa del Caribe como un nuevo reporte para Costa Rica. Basándose en sus características morfológicas y en el análisis molecular de COI y 18S, *H. delta* se traslada aquí al género *Myxia*.

**Palabras clave:** Cixiidae, taxonomía, chicharrita, palmera, Costa Rica

### Introduction

*Myxia* Bahder & Bartlett, 2019 is a monotypic genus recently established to accommodate *Myxia belinda* Bahder & Bartlett, 2019 in Bahder *et al.*, 2019 discovered on palms in Costa Rica (Bahder *et al.* 2019a). This species was discovered surveying planthoppers on palms because of a renewed interest in their host/vector relationships. *Haplaxius*

*crudus* (Van Duzee, 1907) has long been asserted to be involved in the transmission of lethal yellowing (LY) phytoplasmas (e.g., Howard & Thomas 1980) and the recent introduction of lethal bronzing (LB) in Florida (Harrison *et al.* 2008). Skepticism regarding the role of *Haplaxius crudus*, and the general expectation that other planthopper species are involved in vectoring palm diseases has driven further survey of planthoppers on palms.

*Myxia* is allied with *Haplaxius* Fowler, 1904 and *Myndus* Stål, 1862, but distinct based on molecular and morphological evidence. Historically, *Haplaxius* and *Myndus* had been synonyms (e.g., Kramer 1979) but were revised to genus-level status by Emeljanov (1989). Functionally *Haplaxius* is New World and *Myndus* Old World, diagnosed by the absence (*Haplaxius*) or presence (*Myndus*) of a denticle on the forecoxae and carinae terminating on the ventro-lateral corner of the prothorax (*Haplaxius*) or approximately midway (*Myndus*). Interestingly, *Myxia* lacks the denticle observed in *Myndus* but possesses carinae on the pronotum that terminate on the ventral-lateral margin of the pronotum.

The terminalia in *M. belinda* are distinctive. Compared with species of *Haplaxius* considered by Kramer (1979), the presence of a subtriangular medioventral process of the pygofer, bilobed gonostyli, and simple aedeagus subtended by a complex periandrium ( $\approx$ phallobase) appeared unique to *M. belinda* relative to *Haplaxius*. *Haplaxius delta* (Kramer, 1979) (from Guatemala, Belize and Panama) appears to be the most similar (Bahder *et al.* 2019a). Despite distinct molecular and morphological differences in the terminalia between *Myxia* and *Haplaxius*, the two genera appear very similar in the field, especially to *H. crudus*, because of its similar behavior and occurrence on palms. These similarities highlight that there may be other *Haplaxius*-like species on palms that are undescribed (and possibly assumed to be *H. crudus* in the field).

Herein, we describe a novel species of *Myxia* collected from palms. We obtained the cytochrome *c* oxidase subunit I (COI) and 18S genes of the new species and for *Haplaxius delta*, here reported for the first time from Costa Rica, for phylogenetic analyses with other members of the tribe Oecleini.

## Materials and methods

**Locality and specimen collection.** Individuals of the novel taxon were collected from a palm (Arecaceae) belonging to the genus *Geonoma* Willd., 1805 (Fig. 1) in the Reserva Privada el Silencio de Los Angeles Cloud Forest in Costa Rica at the Hotel Villa Blanca, Alajuela Province (10.203231, -84.485094). Specimens were aspirated directly from the palms and transferred to 95% ethanol in the field while still alive. After a few minutes of disturbance, individuals became more active and were subsequently collected by sweep net. Specimens were collected (permit no. SINAC-ACTo-GASPPNI-016-2018) with permission of the Hotel Villa Blanca management and staff and exported under permit number DGVS-256-2018 to the U.S.A. and imported under permit number P526-170201-001. Additionally, a specimen identified in the field as a *Haplaxius* species was collected from a coconut palm in Manzanilla, along the Caribbean coast near the Panamanian border. All specimens collected were measured, photographed and dissected using a Leica M205 C stereoscope. Images of specimens and all features photographed were generated using the LAS Core Software v4.12. Voucher specimens, including primary types, are stored at the University of Florida—Fort Lauderdale Research and Education Center (FLREC) in Davie, FL, U.S.A and the Florida State Collection of Arthropods (FSCA) in Gainesville, FL, U.S.A.

**Morphological terminology and identification.** Morphological terminology generally follows Kramer (1979) except with male terminalia nomenclature updated after Bourgoïn (1988) and Bourgoïn & Huang (1990) and forewing venation following Bourgoïn *et al.* (2015). New taxa are to be attributed to Bahder and Bartlett.

**Dissections and DNA extraction.** The terminalia that were dissected also served as the source of tissue for DNA extraction. The terminal end of the abdomens was removed and placed directly into a solution of tissue lysis buffer (buffer ATL) and proteinase K (180  $\mu$ l ATL and 20  $\mu$ l proteinase K) from the DNeasy<sup>®</sup> Blood and Tissue Kit (Qiagen). The abdomen was left to lyse for 24 hours at 56°C. Following lysis, eluate was transferred to a new 1.5 ml microcentrifuge tube and DNA extraction proceeded as per the manufacturer's instructions. The terminalia were then immersed in 200  $\mu$ l of buffer ATL and 200  $\mu$ l of buffer AL from the same kit and placed at 95°C for 24 hours to remove fat, wax, and residual tissue. The cleared genitalia were then used for morphological characterization and photography.

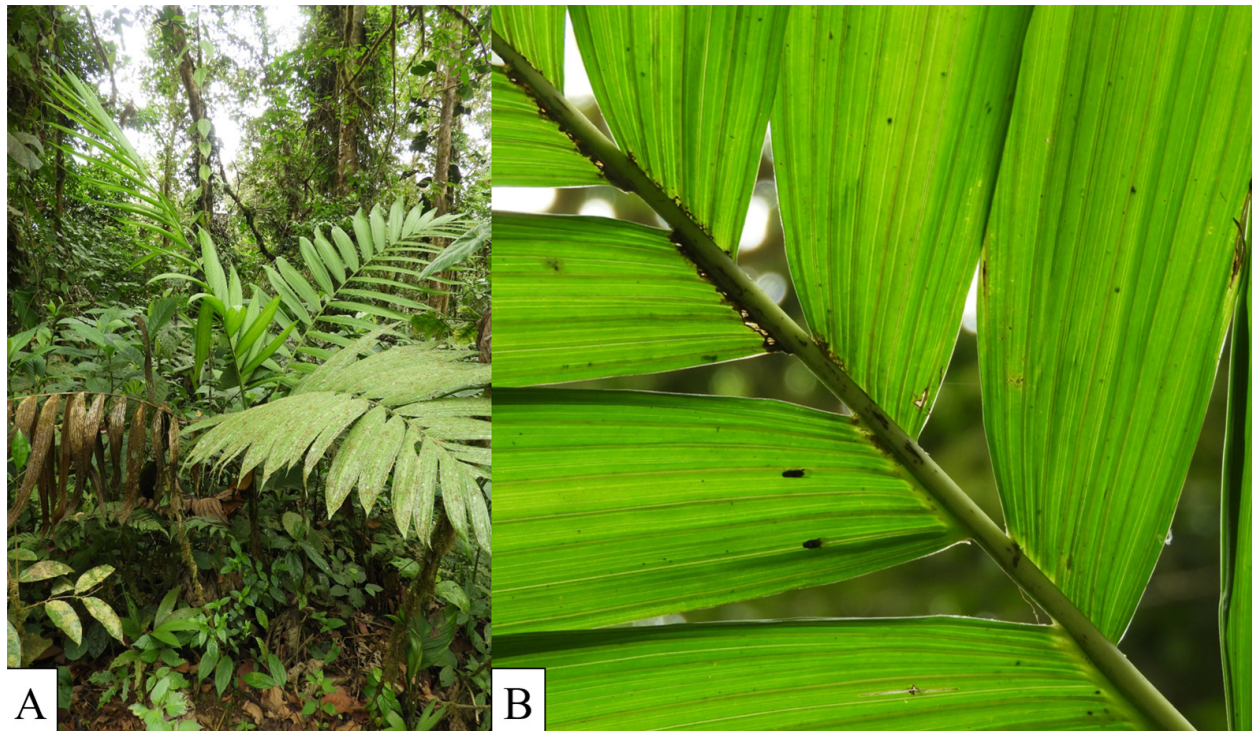


**FIGURE 1.** Habitat and host plant in Los Angeles Cloud Forest where *Myxia baynardi* sp. n. was collected (A) and close-up of *Myxia baynardi* sp. n. *in vivo* (B).

**PCR parameters, sequence data, and analysis.** To obtain COI sequence data, DNA template from specimens was amplified using the primers TYJ1460 (5'-TAC AAT TTA TCG CCT AAA CTT CAG CC-3') and HCO2198 (5'-TCA GGG TGA CCA AAAAAA TCA-3') (Folmer *et al.* 1994). To obtain 18S sequence data, the primers developed by Bahder *et al.* (2019b) were used and are as follows: forward primer 18SF (5'-ACT GTC GAT GGT AGG TTC TG-3'), reverse primer 18SR (5'-GTC CGA AGA CCT CAC TAA A-3'). PCR reactions contained 5x GoTaq Flexi Buffer, 25 mM MgCl<sub>2</sub>, 10 mM dNTP's, 10 mM of each primer, 10% PVP-40, and 2.5U GoTaq Flexi DNA Polymerase, 2 µl DNA template, and sterile dH<sub>2</sub>O to a final volume of 25 µL. Thermal cycling conditions for COI were as follows: 2 min initial denaturation at 95°C, followed by 35 cycles of 30 sec denaturation at 95°C, 30 sec annealing at 40°C, 1 min 30 sec extension at 72°C, followed by a 5 min extension at 72°C. Thermal cycling conditions for 18S were as follows: 2 min initial denaturation at 95°C, followed by 35 cycles of 30 sec denaturation at 95°C, 30 sec annealing at 45°C, 2 min extension at 72°C, followed by a 5 min extension at 72°C. To obtain COI for *M. belinda*, a degenerate forward primer was designed using available COI data from cixiids in the tribe oecleini in GenBank resulting in the forward primer COI\_D1\_F (5'-GGAACWATAAGAAGWATAATYATYCG-3') and the reverse primer was the reverse complement of the C1-J-2195 primer by Simon *et al.* (1994), resulting in the sequence (5'-ACTTCTGGATGACCAAAAAATCAA-3'). Thermal cycling conditions were as follows: 2 min initial denaturation at 95°C, followed by 35 cycles of 30 sec denaturation at 95°C, 30 sec annealing at 40°C, 1 min 30 sec extension at 72°C, followed by a 5 min extension at 72°C. PCR products of the appropriate size were purified using the ExoSAP-IT™ Express PCR Product Cleanup Reagent per the manufacturers' protocol (ThermoFisher Scientific, Waltham, Massachusetts, USA). Purified PCR product was quantified using a NanoDrop Lite Spectrophotometer (ThermoFisher Scientific, Waltham, Massachusetts, USA) and sequenced using the SeqStudio Genetic Analyzer (Applied Biosystems). Contiguous files were assembled using DNA Baser (Version 4.36) (Heracle BioSoft SRL, Pitesti, Romania), aligned using ClustalW as part of the package MEGA7 (Kumar *et al.* 2016). A matrix of pairwise differences using number of differences among COI and 18S was calculated with MEGA7 (Kumar *et al.* 2016). The bootstrap method was used for variance estimation at 1,000 replicates and using the p-distance model. Maximum Likelihood trees were generated using the Bootstrap method at 1,000 replicates based on the Tamura-Nei model for both the COI and 18S loci as well as the consensus tree with concatenated data for COI and 18S data.

**Taxon sampling.** For the COI locus, *Myxia belinda* was used for in-group comparison and out-groups included four species of *Haplaxius*—*H. crudus* Van Duzee, *H. delta* Kramer, *H. dougwalshi* Bahder & Bartlett, 2020 in



Bahder *et al.*, 2020, *H. pictifrons* (Stål, 1862), and *H. skarphion* (Kramer, 1979) and one species of *Oecleus*—*O. mackaspringi* Bahder & Bartlett, 2019 in Myrie *et al.*, 2019). For the 18S locus, *M. belinda* was used for in-group comparison and out-groups included five species of *Haplaxius*—*H. crudus*, *H. delta*, *H. dougwalshi*, *H. pictifrons* Stål, and *H. skarphion*, *Nymphomyndus caribbea* (Fennah, 1971) and *Oecleus mackaspringi*. All in-group and out-group taxa data, including GenBank accession numbers are presented in Table 1.

**TABLE 1.** Taxon sampling of Oecleini for Molecular analysis.

Taxon	Locality	GenBank Accession No.		Collection
		COI	18S	
<i>Haplaxius crudus</i>	Costa Rica	MT080284	MT002393	FLREC
<i>Haplaxius delta</i>	Costa Rica	MT900602	MT892907	FLREC
<i>Haplaxius dougwalshi</i>	Costa Rica	MT080284	MT002395	FLREC
<i>Haplaxius pictifrons</i>	Delaware	MT946292	MN200098	FLREC
<i>Haplaxius skarphion</i>	Costa Rica	MT900603	MT892907	FLREC
<i>Myxia baynardi</i> <b>sp. n.</b>	Costa Rica	MT900604	MT892909	FLREC
<i>Myxia belinda</i>	Costa Rica	MT900605	MN200095	FLREC
<i>Nymphomyndus caribbea</i>	Jamaica	MT080286	MT002394	FLREC
<i>Oecleus mackaspringi</i>	Jamaica	MN488999	MN422261	FLREC

## Results

**Sequence Data.** A 1,308 bp region was amplified and sequenced for the 18S locus (GenBank Accession No. MT892909) for the new species, described below as *Myxia baynardi* **sp. n.** Additionally, a 1,330 bp region was amplified for the 18S locus a specimen of *H. delta* also collected on Costa Rica (GenBank Accession No. MT892908) and *Haplaxius skarphion* (GenBank Accession No. MT892907). Based on the pairwise comparison, *Myxia baynardi* **sp. n.** differed by 0.8% from *M. belinda*. (Table 2). When compared to other genera within the Oecleini, *M. baynardi* **sp. n.** differed on average by 2.2%, 2.5% and 2.7% respectively for *Haplaxius*, *Nymphomyndus*, and *Oecleus* (Table 2). The difference between *H. delta* and *M. belinda* and *M. baynardi* **sp. n.** was 0.8% and 1.3% respectively. Furthermore, *H. delta* differed from other members of *Haplaxius* by an average of 2.0% (range=1.8–2.4%), whereas species within *Haplaxius* differed from each other on average by about 0.7% (range=0.4–1.1%). The phylogenetic analysis provided strong bootstrap support (98) for *M. baynardi* **sp. n.** being closer to *M. belinda* than the other genera of oecleines tested based on the 18S locus (Fig. 2A). Interestingly, *H. delta* resolved with very strong bootstrap support (99) in the *Myxia* clade rather than the *Haplaxius* clade (Fig. 2).

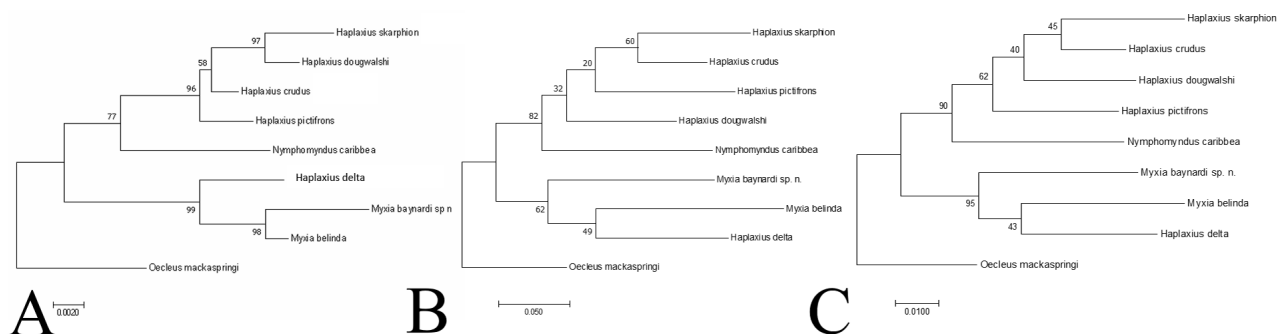


**FIGURE 2.** Maximum likelihood phylogenetic trees (1,000 replicates) giving phylogenetic position of *Myxia baynardi* **sp. n.** relative to related taxa in Oecleini based on the; (A) 18S gene, (B) COI gene and (C) a consensus tree based on concatenated COI and 18S data.

For the COI gene, a 607 bp region was amplified and sequenced (GenBank Accession No. MT900604) for *Myxia baynardi* **sp. n.** and a 615 bp region generated for *H. delta* (GenBank Accession No. MT900602). In addition, the five-prime end of COI for *M. belinda* was amplified and sequenced, yielding at 615 bp sequence (GenBank Acces-

sion No. MT900605) and the five prime end of COI for *H. skarphion* (GenBank Accession No. MT900603). *Myxia baynardi* sp. n. differed by 21.6% from *M. belinda* (Table 3). When compared to other genera within the Oecleini, *M. baynardi* sp. n. differed on average by 20.6%, 17.7% and 19% *Nymphomyndus*, *Oecleus*, and *Haplaxius*, respectively (Table 3). While bootstrap support for placement of the novel taxon was moderate (62) based on COI (Fig. 2B), the consensus tree generated with COI/18S data showed strong support (95) for the placement of *Myxia baynardi* sp. n. in the genus. In all three phylogenies generated, *H. delta* resolved within the *Myxia* clade (Fig. 2)

**TABLE 2.** Pairwise comparison for the 18S gene based on 1,000 bootstrap replications using the p-distance method; numbers on bottom left=percent difference, numbers in upper right=standard error.

	1	2	3	4	5	6	7	8	9
1 <i>Myxia baynardi</i> sp. n.		0.002	0.003	0.004	0.005	0.004	0.004	0.004	0.005
2 <i>Myxia belinda</i>	0.008		0.002	0.003	0.004	0.004	0.004	0.004	0.004
3 <i>Haplaxius delta</i>	0.013	0.008		0.003	0.004	0.004	0.003	0.004	0.004
4 <i>Haplaxius pictifrons</i>	0.023	0.019	0.020		0.003	0.003	0.002	0.003	0.004
5 <i>Haplaxius skarphion</i>	0.029	0.025	0.024	0.011		0.002	0.002	0.004	0.004
6 <i>Haplaxius dougwalshi</i>	0.025	0.021	0.019	0.008	0.006		0.002	0.004	0.004
7 <i>Haplaxius crudus</i>	0.022	0.018	0.018	0.004	0.008	0.005		0.003	0.004
8 <i>Nymphomyndus carribea</i>	0.025	0.021	0.021	0.013	0.017	0.016	0.012		0.004
9 <i>Oecleus mackaspringi</i>	0.027	0.023	0.023	0.019	0.025	0.021	0.019	0.021	

**TABLE 3.** Pairwise comparison for the COI gene based on 1,000 bootstrap replications using the p-distance method; numbers on bottom left=percent difference, numbers in upper right=standard error.

	1	2	3	4	5	6	7	8	9
1 <i>Myxia baynardi</i> sp. n.		0.018	0.015	0.016	0.017	0.015	0.016	0.017	0.016
2 <i>Myxia belinda</i>	0.216		0.017	0.017	0.016	0.017	0.017	0.016	0.016
3 <i>Haplaxius delta</i>	0.175	0.187		0.015	0.015	0.017	0.016	0.016	0.016
4 <i>Haplaxius pictifrons</i>	0.189	0.213	0.179		0.014	0.015	0.015	0.015	0.016
5 <i>Haplaxius skarphion</i>	0.203	0.182	0.179	0.155		0.015	0.013	0.014	0.016
6 <i>Haplaxius dougwalshi</i>	0.187	0.199	0.194	0.150	0.153		0.013	0.015	0.015
7 <i>Haplaxius crudus</i>	0.196	0.204	0.189	0.141	0.112	0.124		0.015	0.016
8 <i>Nymphomyndus carribea</i>	0.206	0.211	0.201	0.169	0.164	0.174	0.170		0.016
9 <i>Oecleus mackaspringi</i>	0.177	0.194	0.196	0.199	0.175	0.167	0.179	0.189	

## Systematics

### Family Cixiidae Spinola, 1839

### Subfamily Cixiinae Spinola, 1839

### Tribe Oecleini Muir, 1922

### Genus *Myxia* Bahder & Bartlett, 2019

Type species: *Myxia belinda* Bahder & Bartlett, 2019; by monotypy and original designation.

**Diagnosis.** Vertex longer at midline than wide, median carina present, evanescent distally. Hind tibiae lacking spines, forecoxae lacking denticle. Lateral pronotal carinae terminating on ventral margin of prothorax, tegulae evident. Medioventral process of the pygofer is subtriangular. Parameres distally bifid in lateral view and acute apex in ventral view with inner lateral tooth near apex. Periandrium ( $\approx$ phalobase) usually ring-like at base of aedeagus,

prolonged into a projection of varying form subtending the aedeagus. Anal tube short and stout, distally projecting ventrally of ventrocaudally.

**Remarks.** Bahder *et al.* (2019a) noted that the terminalia of *H. delta* resembled those of *Myxia belinda* based on the illustrations of Kramer (1979) (specimens were not then available). Serendipitously, a specimen of *H. delta* was collected in Costa Rica. The resulting morphological comparison and molecular analysis gives strong support for transferring *H. delta* to *Myxia*, bringing the species count to three; *M. baynardi* **sp. n.**, *M. belinda*, and *M. delta* (Kramer, 1979) **new combination**. The genus is now further supported with strong molecular support and consistent morphological characters among three taxa.

Based on a combination of molecular and morphological evidence we place *Haplaxius delta* in *Myxia* as *Myxia delta* (Kramer, 1979) **new combination**. Both COI and 18S phylogenies have support for the genus *Myxia* as a clade (99 and 62 bootstrap support respectively with the consensus tree also providing support (95 bootstrap support). In all cases, *H. delta* resolved within the *Myxia* clade (Fig. 10). Furthermore, the general form of the parameres, ventral process of the pygofer, and aedeagus are consistent with the type species, *Myxia belinda*.

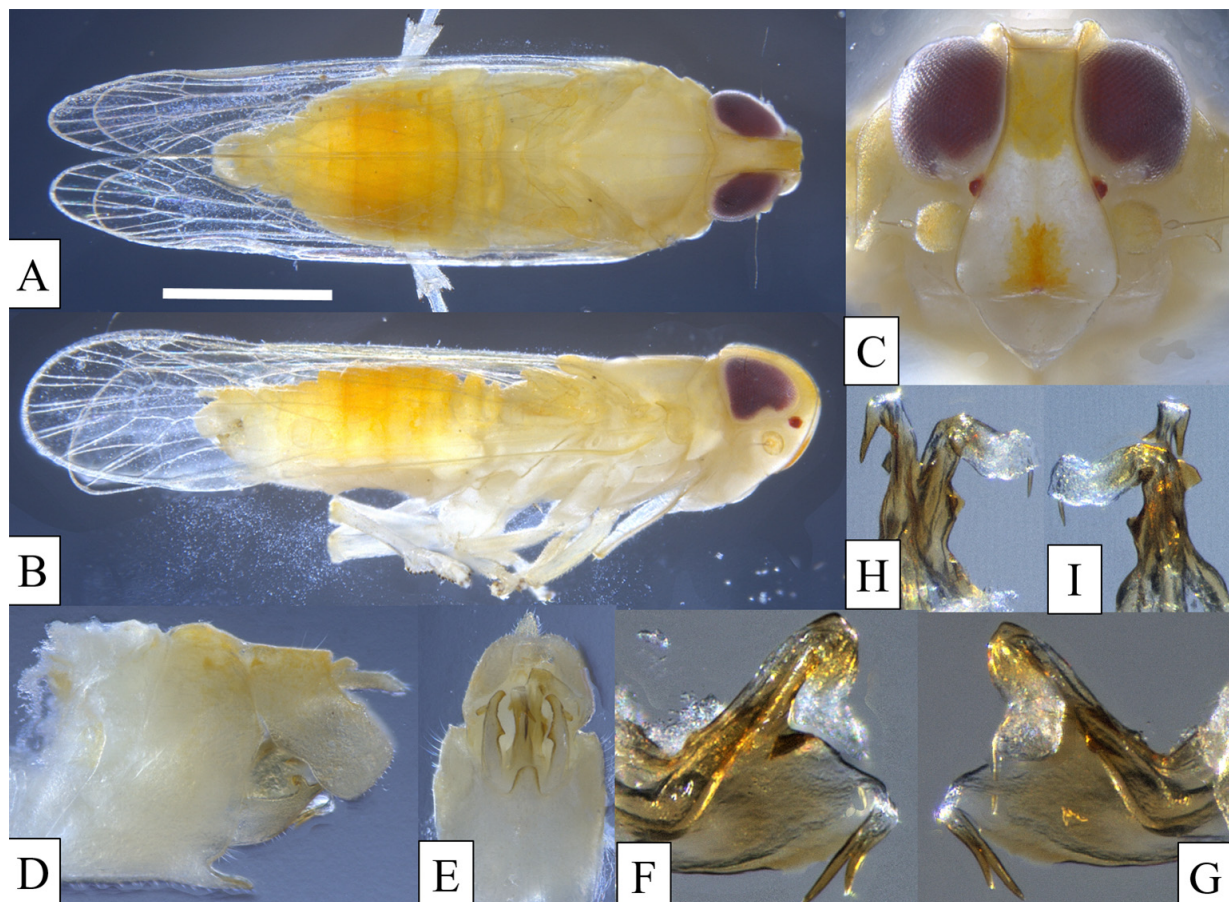


**FIGURE 3.** *Myxia delta* (Kramer): (A) Habitus, dorsal view, (B) lateral view, (C) habitus frontal view, (D) terminalia lateral view, (E) terminalia ventral view, (F) aedeagus and periandrium left lateral view; (G) aedeagus and periandrium right lateral view, (H) aedeagus and periandrium ventral view, and (I) aedeagus and periandrium dorsal view.

### *Myxia baynardi* **sp. n.**

(Figures 4–11)

**Type locality.** Costa Rica, Alajuela, Reserva Privada el Silencio de Los Angeles, Hotel Villa Blanca.

**Diagnosis.** Body color dark fuscous. Basal third of forewing fuscous with conspicuous pterostigma. Vertex bicolored (fuscous anteriorly, pale caudad), relatively broad and flat. Gonostyli in ventral view strongly curved inward. Aedeagal shaft stout, aedeagus plus flagellum curled nearly into complete helix, bearing four processes on left lateral side (last two paired). Periandrium ring-like at base of aedeagus with elongate projection subtending aedeagus bearing two elongate, strongly hooked apical processes.



**Description.** *Color.* General body color dark brown. Fore and middle legs light brown and hind legs testaceous (Fig. 4A & 4B). Head with vertex bicolored, caudally tan, distally dark brown; frons dark brown, except pale marks above lateral portion of frontoclypeal suture; upper half of clypeus and genae below antennae white, grading to brown below (Fig. 5A–5C). Pronotum chestnut-brown. Mesonotum dark brown anteriorly becoming paler posteriorly with scutellum white (except brown adjacent to scutum; Fig. 5A). Forewings distally clear, proximally darkened in proximal third of forewings plus brown patch along Sc+R vein to pterostigma (veins embrowned to wing midlength); middle of costal cell and basal half of clavus up to CuP light fuscous (Fig. 6A). Abdomen dark brown (reddish brown in females).

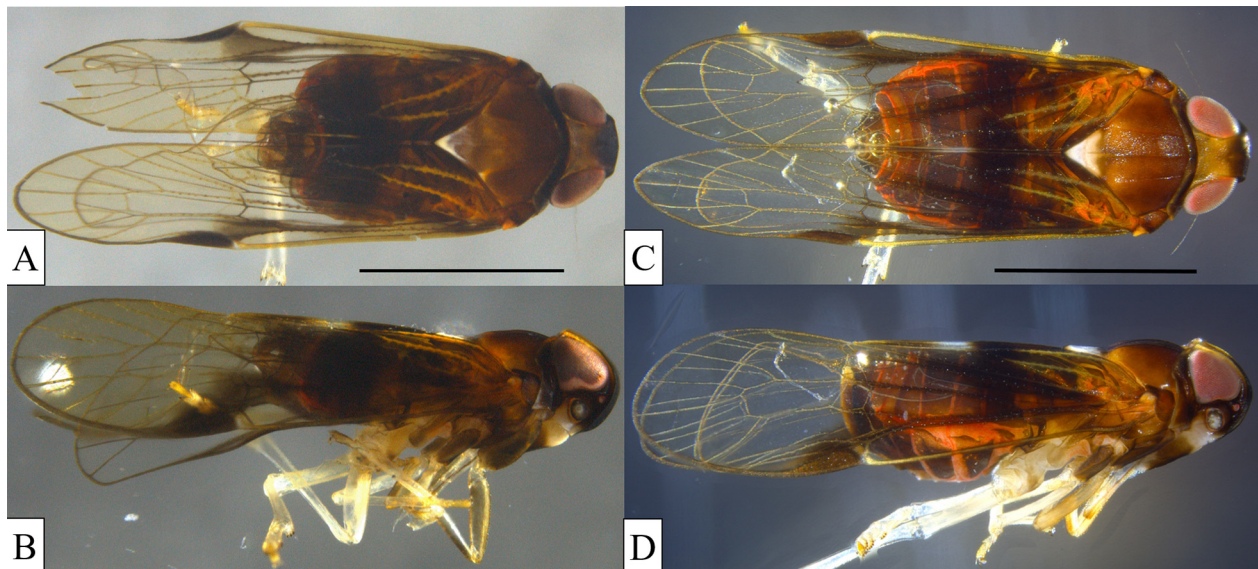


**FIGURE 4.** Adult habitus *Myxia baynardi* sp. n.; (A) body dorsal view male, (B) body lateral view male, (C) body dorsal view female, and (D) body lateral view female, scale = 1 mm.

*Structure.* Body length males with wings ( $n = 4$ ): 2.62–2.81 mm; males without wings 1.74–1.75 mm; females with wings ( $n = 18$ ): 3.33–3.54 mm; females without wings 2.25–2.26 mm. Head. Head in lateral view obtusely rounded (Fig. 5B). Vertex (dorsal view) roughly quadrate, length males: 0.22–0.23 mm, females: 0.24–0.25 mm; width at hind margin males: 0.30–0.31 mm; females: 0.33–0.35 mm; width at distal margin males: 0.19–0.20 mm; females: 0.22–0.24 mm; median carina nearly obsolete (strongest near posterior margin), broadest caudally, weakly narrowing distally (expanded slightly at apex) to weakly convex apex; fastigium (lateral view), smoothly rounded, bearing weak transverse carina (Fig. 5A). Frons broadly ovate, longer than wide, length males: 0.39–0.40 mm, females: 0.41–0.42 mm; dorsal width males: 0.19–0.20 mm, females: 0.21–0.22 mm; width at widest point males: 0.30–0.31 mm, females: 0.32–0.34 mm; frontoclypeal margin width, males: 0.28–0.29 mm; females: 0.30–0.31 mm; sides laterally carinate, convexly arched, narrowest and parallel-sided between eyes, expanding ventrally about to level of antennae, constricting at frontoclypeal suture, median carina evident, median ocellus distinct (Fig. 5B). Lateral ocelli conspicuous on genae below eyes at level of top of antennae; antennae bulbous, scape very short, pedicel about as wide as tall bearing conspicuous sensory plaques, flagellum bristle-like with bulbous base. Clypeus roughly triangular, median carina evident, length males: 0.12–0.13 mm; females: 0.14–0.16 mm.

Thorax. Pronotum short, length at midline males: 0.03–0.04 mm; females: 0.04–0.05 mm; convex anteriorly, concave posteriorly, roughly uniform width from midpoint to tegulae (Fig. 5A); median carina weak; postocular pronotal carinae almost obsolete, extending to ventral margin, approximate midpoint (Fig. 7). Mesonotum slightly longer than wide; length at midline males: 0.54–0.55 mm; females: 0.55–0.56 mm; width males: 0.57–0.58 mm; females: 0.58–0.59 mm; tricarinate, lateral carinae, diverging posteriorly, reaching posterior margin (Fig. 5A).

Forewing (Fig. 7) length males: 2.18–2.19 mm; females: 2.21–2.22 mm; bearing conspicuous pterostigma; veins punctate with setal bases (more conspicuous proximally); clavus reaching midlength, about level of Sc and fork of CA; fork of R proximal to apex of clavus. Branching pattern: RA one-branched, RP three-branched, MP four-branched, CuA two-branched (converging to form small C5 cell); fusion of Pcu and A1 in clavus near claval midlength.

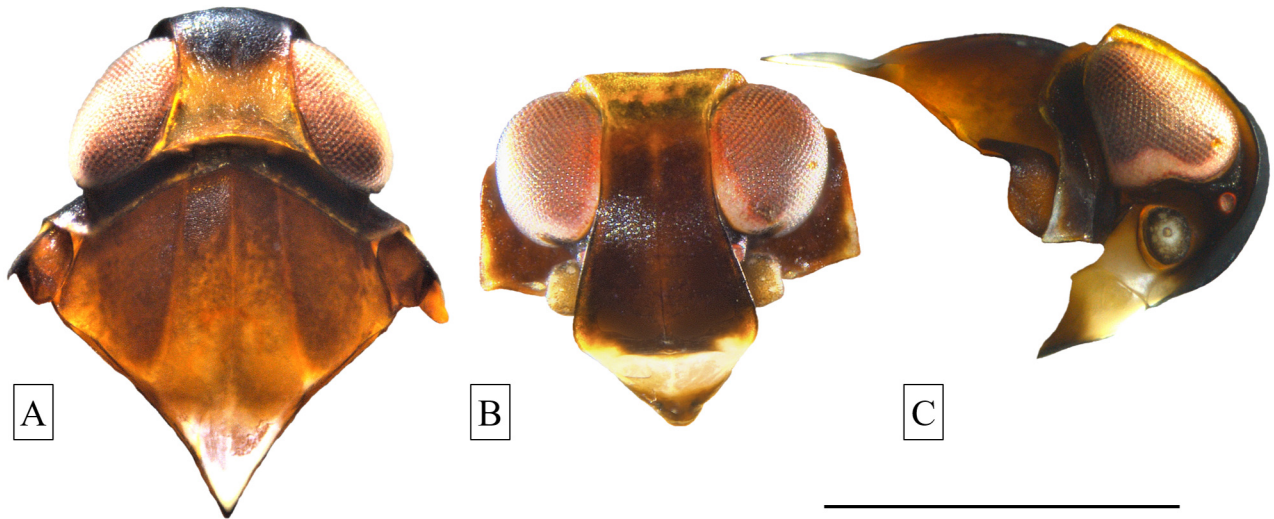


**FIGURE 5.** Adult *Myxia baynardi* sp. n.: (A) male head, pronotum, and mesonotum dorsal view, (B) male head and pronotum frontal view, and (C) male head, pronotum and mesonotum lateral view, scale = 1 mm.

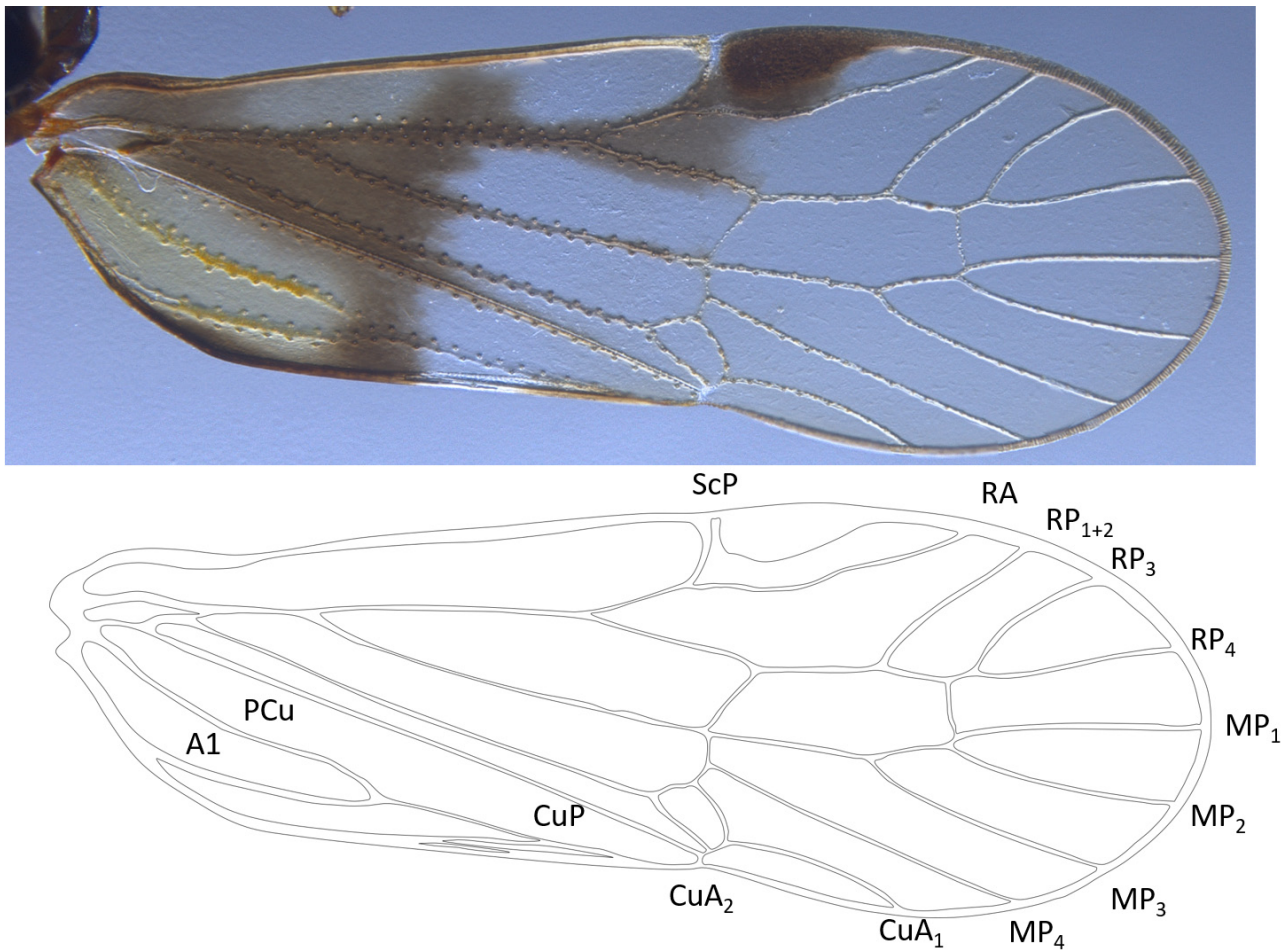


**FIGURE 6.** Forewing venation of *Myxia baynardi* sp. n.

**Terminalia.** Pygofer in lateral view roughly triangular, broadest basally, narrowing dorsally; anterior margin concave, posterior margin sinuate, with distinct subbasal concavity (Fig. 8A); sides of pygofer with ridge (marking slight inward inflection of pygofer) arising from posterior margin in dorsal fourth, arching ventrad back to posterior margin at top of subbasal concavity, forming an irregular half-circle (Figs. 8A & 8B). In ventral view, ventral opening of pygofer with bluntly triangular medioventral lobe, terminating at rounded, knob-like apex (Fig. 8B).



Gonostyli in lateral view (Fig. 8A & 9) narrow basad, expanding midpoint, constricting with dorsal margin slightly serrate (Fig. 9), apex broadly rounded with an anteriorly angled dorsal process (Fig. 9); in ventral view, widest at base, strongly incurved, constricting distally, bearing subapical inner lateral tooth (Fig. 8B). Periandrium basally ring-like, not extending dorsally (Fig. 10C) but strongly developed ventrally as a ventral prolongation bearing 2 long acute processes; supporting dorsally an elongated well sclerotized aedeagus (enclosing ductus ejaculatorius). Aedeagal shaft (lateral view) simple, irregularly sinuate on dorsal and ventral margin (Fig. 10), distally downcurved; sclerotized aedeagus plus membranous endosoma collectively arced into sinistral helix; entire structure roughly segregated into three parts, the thicker, sclerotized basal third and second a thinner sclerotized portion (collectively comprising the aedeagus), with a simple distal membranous endosomal apex (forming a membranous tubular sac); the downward directed distal portion of the aedeagus bearing 4 elongate processes (Fig. 10A), one arising near flagellar base on left ventro-lateral side (F1), a second arising on the left dorso-lateral margin (F2), and a terminal pair (F3 & F4) directed anteriorly from a common base (F3 & F4), both slightly curved, F3 dorsal, F4 ventral (Fig. 10 & Fig. 11). Anal segment (lateral view) short, broad, spatulate with downcurved, broadly rounded apex (Fig. 8A); in dorsal view, approximately as long as wide, lateral margins nearly parallel, apex irregularly rounded (Fig. 8C); paraproct in dorsal view, short and conical.

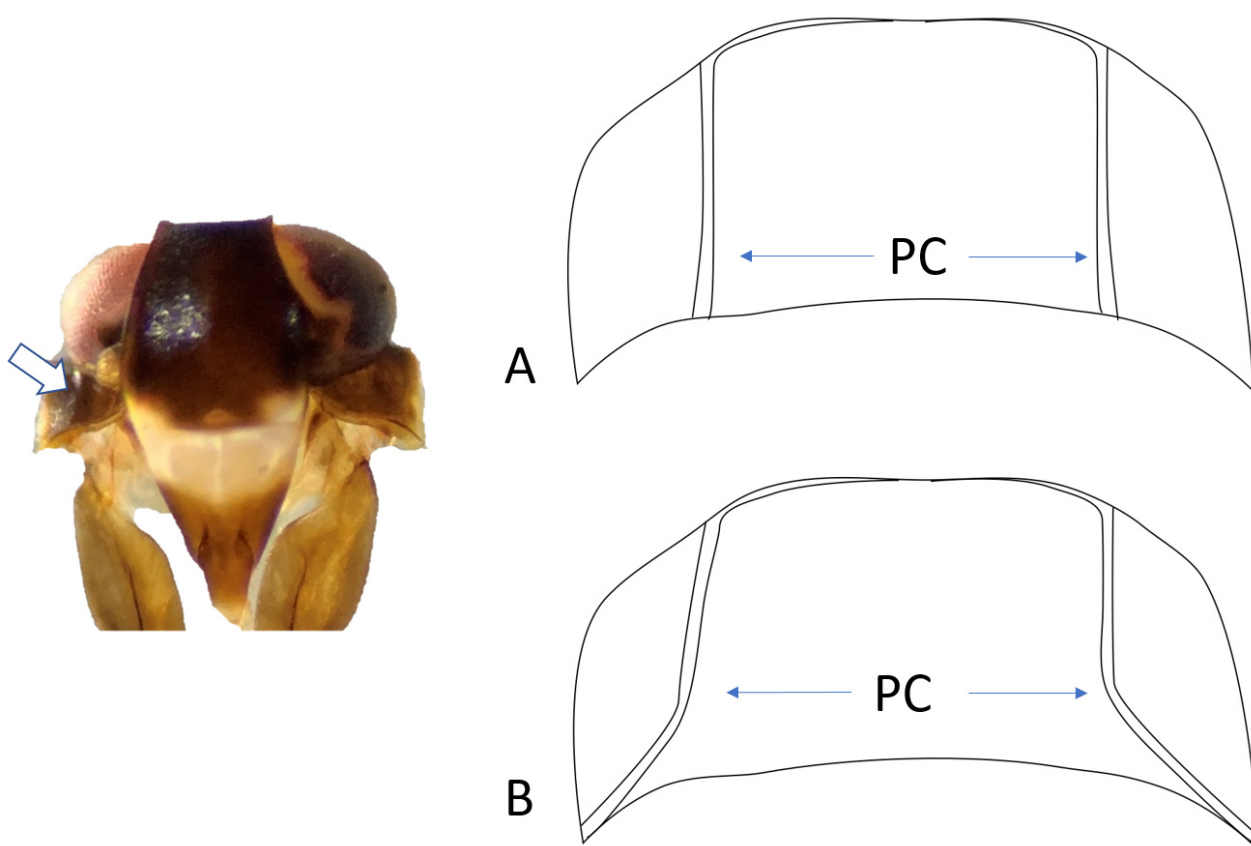


**FIGURE 7.** Habitus frontal view highlighting presence (white arrow) of carina on prothorax that terminates at midpoint of ventral margin of prothorax; illustration of generalized prothorax in frontal view highlighting the pronotal carinae (PC) orientation in *Myxia* and *Myndus* (A) and in *Haplaxius* (B).

**Plant associations.** Palm (*Geonoma* sp.), Arecaceae.

**Distribution.** Costa Rica (Alajuela).

**Etymology.** The specific name is given in honor of the senior author's father, James Herbert Bahder, who was commonly called "Baynard" by friends and family.

**Material examined.** Holotype male "Costa Rica, Alajuela / Los Angeles Cloud Forest / Coll.: B.W.Bahder / 16.V.2018 / Host: *Geonoma* sp. palm // Holotype / *Myxia baynardi*" (FSCA) Paratypes, Los Angeles Cloud Forest [16 May 2018] (3 males, 18 females, FLREC).

**Remarks.** The morphological features of *Myxia baynardi* **sp. n.** that are consistent with the genus *Myxia* especially include the form of the terminalia—having a short, stout, downward directed anal tube, and the periandrium

separated from, and subtending, the aedeagus, in combination with the molecular evidence places this species in *Myxia*. However, *Myxia baynardi* **sp. n.** is dark colored (contrasting with the pale *Myxia belinda* and *Myxia delta*). With a broad, smooth vertex (in contrast to the other two species with a relatively narrow vertex with lateral margins keeled making the vertex disc convex). Furthermore, the form of the aedeagal complex is unusual, having the aedeagus plus endosoma curled into a sinistral helix. Also, the demarcation between the endosoma and aedeagus is not entirely clear—while it is evident that the distal membranous portion is endosoma, it is entirely possible that the preceding sclerotized portion bearing the four processes also is part of the morphological endosoma. We anticipate that additional *Myxia* will be discovered and described in further survey work in the Caribbean basin and it will be of interest to see how this unusual taxon compares morphologically and molecularly to other *Myxia* taxa as they are discovered.

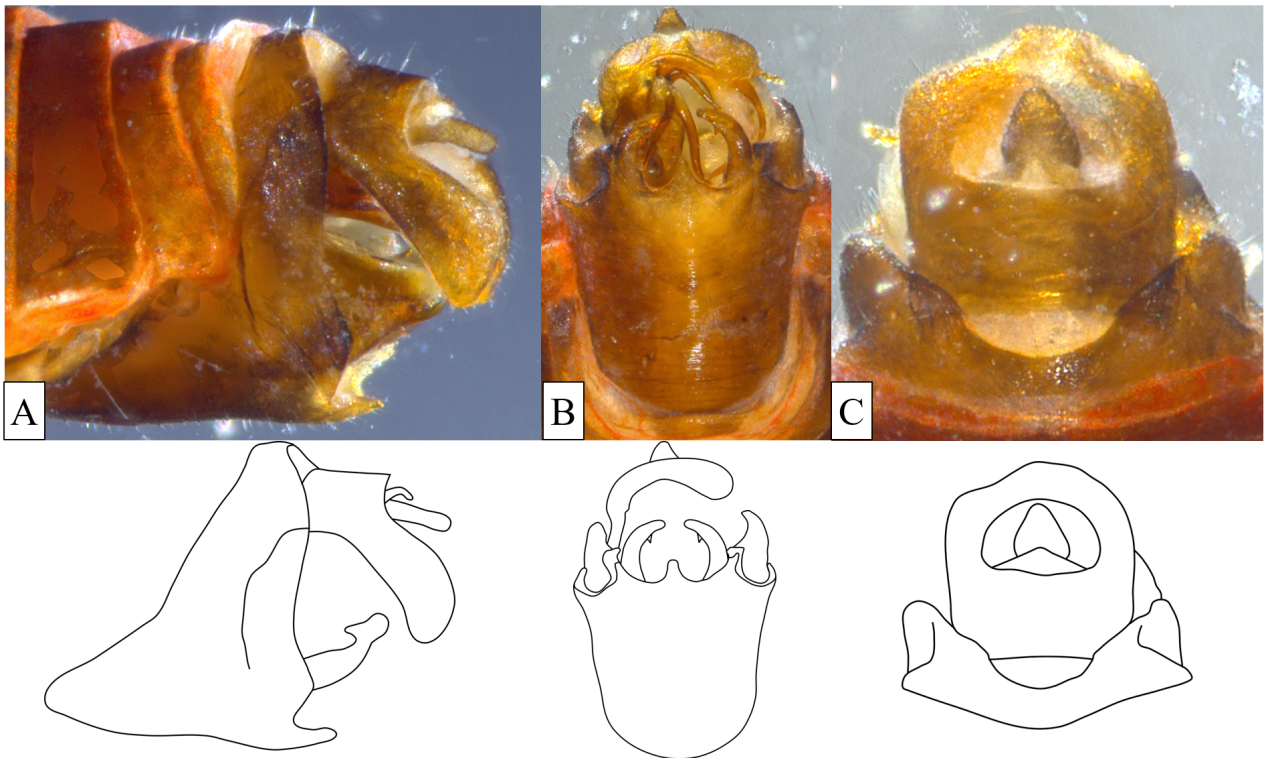


**FIGURE 8.** Male terminalia of *Myxia baynardi* **sp. n.**; (A) lateral view, (B), ventral view, and (C) dorsal view.

### Other species collected

*Myxia delta* (new country record)—“Costa Rica, Limón / Manzanillo, nr. Panama / B.W. Bahder, 14.V.2018 / aspirated from *Cocos nucifera*” (1 male) (Fig. 9).



**FIGURE 9.** Caudo-lateral view of male gonostylus for *Myxia baynardi* **sp. n.**



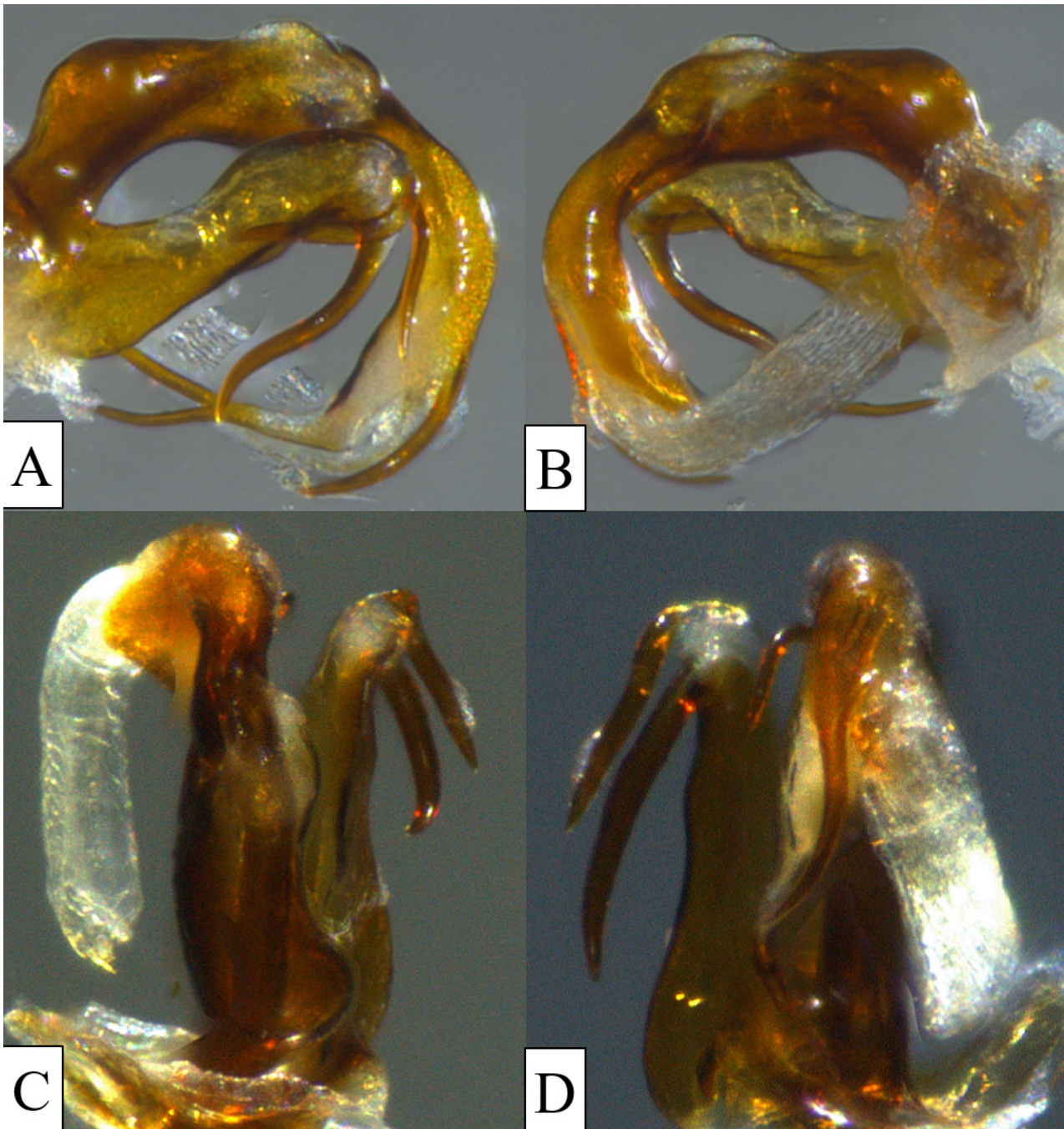


**FIGURE 10.** Aedeagus and periandrium of *Myxia baynardi* sp. n.: (A) right lateral view, (B), left lateral view, (C) dorsal view, and (D) ventral view.

**Key to the species of *Myxia***

- 1. Body dark fuscous, vertex bicolored (tannish caudally, fuscous distally), wings patterned, lacking *ir* crossvein (*im* also missing); flagellum large bearing four long sclerotized processes . . . . . *Myxia baynardi* sp. n.
- 1'. Body testaceous or yellow, vertex pale, not bicolored; wings clear. . . . . 2
- 2. Body uniformly yellow, face without markings, periandrium with large retrose spine and two subapical anterior angled spines . . . . . *Myxia belinda* Bahder & Bartlett
- 2'. Body testaceous, face with white markings and orange patch traversing median carina, periandrium with two apical spines . . . . . *Myxia delta* (Kramer)



## Discussion

The novel taxon, while superficially appears quite different from *M. belinda*, possesses characters of the terminalia that are consistent with its placement in *Myxia*, especially given the molecular support for its placement near *M. belinda* for both COI and 18S. However, *M. baynardi* sp. n. superficially appears fairly different from *M. belinda* and we had initially presumed it to belong to *Haplaxius*. *Haplaxius* as it is currently comprised contains some forms that are superficially similar (e.g., *Haplaxius slossonae* (Ball, 1902)). A possibility we are considering is that *Haplaxius* as currently comprised may be heterogeneous, but at present we have data from too few forms to adequately address this possibility. This distinct differences in color and wing patterns observed may suggest the presence of subgenera, there is not enough data to support this at the moment.

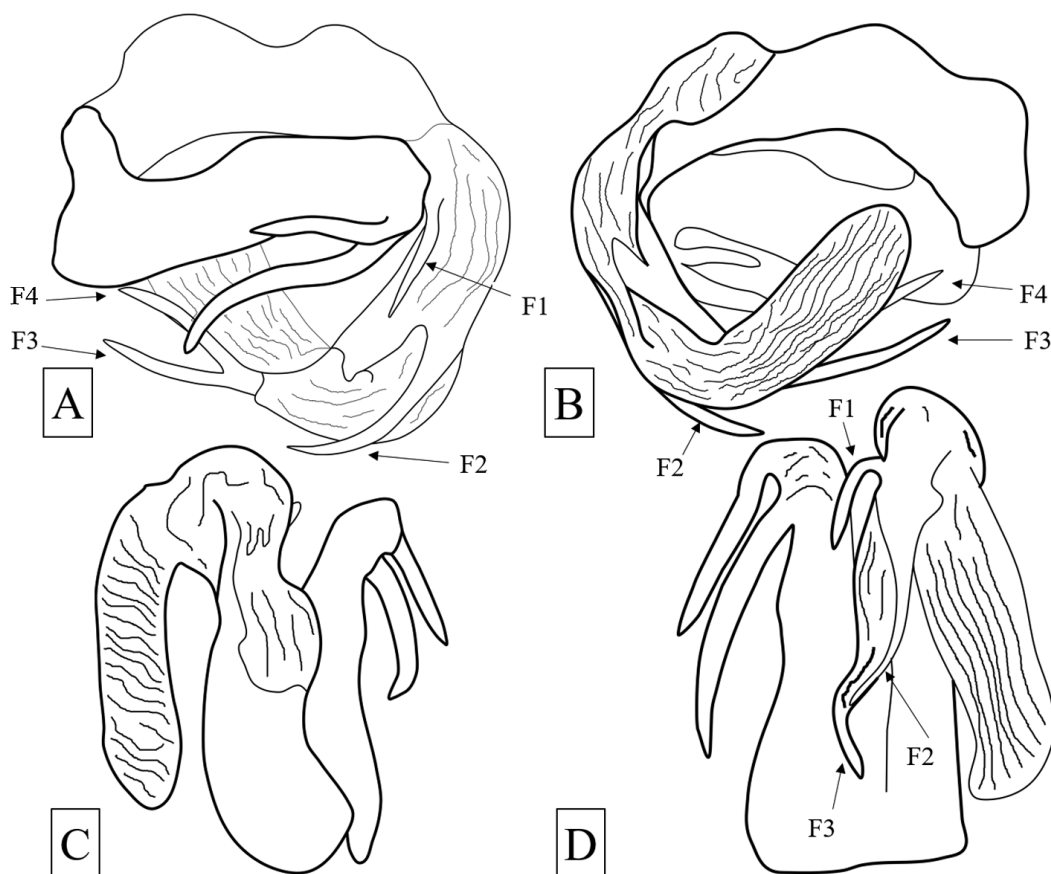


**FIGURE 11.** Line art of aedeagus and perianthium of *Myxia baynardi* sp. n.: (A) right lateral view, (B), left lateral view, (C) dorsal view, and (D) ventral view.

## Acknowledgements

The authors are grateful to staff and management at Hotel Villa Blanca for their ongoing support of this research. The authors are grateful to Luz Bahder for translating the abstract into Spanish. Funding for this research was provided University of Florida—Institute of Food and Agricultural Sciences and Emerging Pathogens Institute for providing seed grant funding to support survey work in Costa Rica.

## References

- Bahder, B.W., Bartlett, C.R., Barrantes, E.A.B., Zumbado, M.A.Z., Humphries, A.R., Helmick, E.E. Goss, E.M. & Ascunce, M.S. (2019a) A new genus and species of cixiid planthopper (Hemiptera: Auchenorrhyncha: Fulgoroidea) from the Reserva Privada el Silencio de Los Angeles Cloud Forest in Costa Rica. *Zootaxa*, 4701 (1), 065–081. <https://doi.org/10.11646/zootaxa.4701.1.5>

- Bahder, B.W., Bartlett, C.R., Barrantes, E.A.B., Echavarría, M.A.Z., Humphries, A.R., Helmick, E.E., Ascunce, M.S. & Goss, E.M. (2019b) A new species of *Omolicna* (Hemiptera: Auchenorrhyncha: Fulgoroidea: Derbidae) from coconut palm in Costa Rica and new country records for *Omolicna brunnea* and *Omolicna triata*. *Zootaxa*, 4577 (3), 501–514.  
<https://doi.org/10.11646/zootaxa.4577.3.5>
- Bahder, B.W., Barrantes, E.A.B., Echavarría, M.A.Z., Mou, D., Helmick, E.E. & Bartlett, C.R. (2020) A new species of planthopper in the genus *Haplaxius* (Hemiptera: Auchenorrhyncha: Fulgoroidea: Cixiidae) on palms in Costa Rica and a new county record for *Haplaxius skarphion*. *Zootaxa*, 4767 (4), 543–553.  
<https://doi.org/10.11646/zootaxa.4767.4.4>
- Ball, E.D. (1902) Some new North American Fulgoridae. *The Canadian Entomologist*, 34, 147–157.  
<https://doi.org/10.4039/Ent34147-6>
- Bourgoin, T. (1988) A new interpretation of the homologies of the Hemiptera male genitalia illustrated by the Tettigometridae (Hemiptera, Fulgoromorpha). In: Vidano, C. & Arzone, A. (Eds.), *Proceedings of the 6th Auchenorrhyncha Meeting, Turin, Italy, 7–11 September 1987*. Consiglio Nazionale delle Ricerche, IPRA Rome, pp. 113–120.
- Bourgoin, T. & Huang, J. (1990) Morphologie compare des genitalia males des Trypetimorphini et remarques phylogénétiques (Hemiptera: Fulgoromorpha: Tropiduchidae). *Annales de la Société entomologique de France*, 26, 555–564.
- Bourgoin, T., Wang, R.R., Ache, M., Hoch, H., Soulier-Perkins, A., Stroinski, A., Yap, S. & Szewo, J. (2015) From micropterism to hyperpterism: recognition strategy and standardized homology-driven terminology of the forewing venation patterns in planthoppers (Hemiptera: Fulgoromorpha). *Zoomorphology*, 134 (1), 63–77.  
<https://doi.org/10.1007/s00435-014-0243-6>
- Emeljanov, A.F. (1989) On the problem of division of the family Cixiidae (Homoptera, Cicadina). *Entomologicheskoe Obozrenie*, 68 (1), 93–106. [in Russian, translated to English in *Entomological Review*, 68 (4), 54–67 (1989)]
- Fowler, W.W. (1904). Order Rhynchota. Suborder Hemipter-Homoptera. (Continued). *Biologia Centrali-Americana; contributions to the knowledge of the fauna and flora of Mexico and Central America*, 1, 85–124.  
<https://doi.org/10.5962/bhl.title.730>
- Harrison, N.A., Helmick, E.E. & Elliott, M.L. (2008) Lethal-yellowing type diseases of palms associated with phytoplasmas newly identified in Florida, USA. *Annals of Applied Biology*, 153 (1), 85–94.  
<https://doi.org/10.1111/j.1744-7348.2008.00240.x>
- Howard, F.W. & Thomas, D.L. (1980) Transmission of palm lethal decline to *Veitchia merrillii* by a planthopper *Myndus crudus*. *Journal of Economic Entomology*, 73 (5), 715–717.  
<https://doi.org/10.1093/jee/73.5.715>
- Folmer, O., Black, M., Hoeh, W., Lutz, R. & Vrijenhoek, R. (1994) DNA primers for amplification of mitochondrial cytochrome *c* oxidase subunit I from diverse metazoan invertebrates. *Molecular Marine Biology and Biotechnology*, 3 (5), 294–299.
- Kramer, J.P. (1979) Taxonomic study of the planthopper genus *Myndus* in the Americas (Homoptera: Fulgoroidea: Cixiidae). *Transactions of the American Entomological Society*, 105 (3), 301–389.  
<http://www.jstor.org/stable/25078242>
- Kumar, S., Stecher, G. & Tamura, K. (2016) MEGA7: Molecular Evolutionary Genetics Analysis version 7.0 for bigger datasets. *Molecular Biology and Evolution*, 33, 1870–1874.  
<https://doi.org/10.1093/molbev/msw054>
- Muir, F.A.G. (1922) New Malayan Cixiidae (Homoptera). *Philippine Journal of Science*, 20, 111–119.
- Myrie, W., Helmick, E.E., Bartlett, C.R., Bertacini, A. & Bahder, B.W. (2019) A new species of planthopper belonging to the genus *Oecleus* Stål, 1862 (Hemiptera: Fulgoroidea: Cixiidae) from coconut palm (*Cocos nucifera* L.) in Jamaica. *Zootaxa*, 4712 (1), 127–137.  
<https://doi.org/10.11646/zootaxa.4712.1.9>
- Simon, C., Frati, F., Beckenbach, A., Crespi, B., Liu, H. & Flook, P. (1994) Evolution, weighting, and phylogenetic utility of mitochondrial gene sequences and a compilation of conserved polymerase chain reaction primers. *Annals of the Entomological Society of America*, 87 (6), 651–701.  
<https://doi.org/10.1093/aesa/87.6.651>
- Spinola, M. (1839) Essai sur les Fulgorelles, sous-tribu de la tribu des Cicadaïres, ordre des Rhyngotes. *Annales de la Société Entomologique de France*, 8, 133–337.
- Stål, C. (1862) Novae vel minus cognitae Homopterorum formae et species. *Berliner Entomologische Zeitschrift*. Berlin, 6, 303–315.
- Van Duzee, E.P. (1907) Notes on Jamaican Hemiptera: A report on a collection of Hemiptera made on the island of Jamaica in the spring of 1906. *Bulletin of the Buffalo Society of Natural Sciences*, Buffalo, New York, 8 (5), 3–79.